

Hybrid modelling and fault current characteristics of PV-integrated power systems

Haichi Tang

Department of Engineering Computer Science Building (K17), University of New South Wales, Kensington, Australia

z5505769@ad.unsw.edu.au

Abstract. The move to Inverter-Based Renewable Resources (IBRs) is a challenge for power system protection since IBRs generate much lower fault currents than traditional synchronous generators. This compromises the operation of conventional protection relays. In order to solve this problem, the present study employs a detailed Institute of Electrical and Electronics Engineers (IEEE) 9-bus model in Real Time Simulation for Computer Aided Design (RSCAD) to examine the fault behaviour at four different levels of renewable energy penetration. The investigation measures the reduction of the fault current as a result of the gradual substitution of synchronous generation by photovoltaics. The findings enable the production of different sets of relay settings for each case, thus assuring the correct functioning of protection coordination in terms of reliability and selectivity. The main point is an extensive adaptive protection concept. This thoughtful plan serves as an essential guide for the dynamic adjustment of relay settings, thus ensuring the resilience and stability of the grid during the energy transition.

Keywords: adaptive protection, Inverter-Based Resources (IBRs), fault current, renewable energy penetration, power system stability

1. Introduction

Photovoltaic (PV) generation is one of the major factors driving the rapid change in distributed power networks. Inverter-Based Resources (IBRs) have the modularity and low emissions that PV offers, but their growing presence has led to significant protection challenges [1]. Traditional protection was designed for systems with synchronous generators, which have predictable fault currents regulated by the machine impedance. PV inverters operate fundamentally differently [2]: their current-limiting controllers generate fault currents that are significantly smaller, shorter in duration, and determined by internal algorithms. As a result of these changed fault signatures, there are misoperations, a decrease in relay sensitivity, and an increase in system reliability issues that have been identified by [3, 4].

The research presented here develops the hybrid RSCAD model framework that captures the dynamic behaviour of PV-integrated systems during faults. By combining physics-based inverter models with equivalent network representations, the study evaluates the impact of PV penetration on the short-circuit

current magnitude, phase angle, and waveform distortion. The main contributions are the comparative simulations and the adaptive protection concepts for the high-IBR networks.

2. System modelling and simulation framework

The chapter outlines the creation of the electromagnetic transient model for a hybrid SG-PV system in RSCAD. For consistency, all parts were modelled on a common per-unit base. In order to depict the changeover of the grid from synchronous to inverter-dominant conditions, three PV penetration levels (10%, 40%, 80%) were considered. The system's reaction to short-circuit faults at various locations was captured through very detailed time-step simulations. The study used these parameters—fault current magnitude, waveform, and phase angle behaviour—to literally measure the impact of increasing PV penetration on system strength and protection performance.

2.1. Hybrid system configuration

Our hybrid model of IEEE 9-bus system, Figure 1, created in RSCAD, is a representative of a modern power grid which has both conventional and renewable generation. The Synchronous Generator (SG) is the conventional power source that stabilises the grid inherently by its rotating mass. The Photovoltaic (PV) Inverter is a controlled current source with quick protection features. These sources are connected through transformers, transmission lines, loads, and busbars which make up the network. All components were of the same parameters (100 MVA, 230 kV base) to provide a uniform system representation throughout the RSCAD simulation platform. Bus data and transmission line details are given in Table 1.

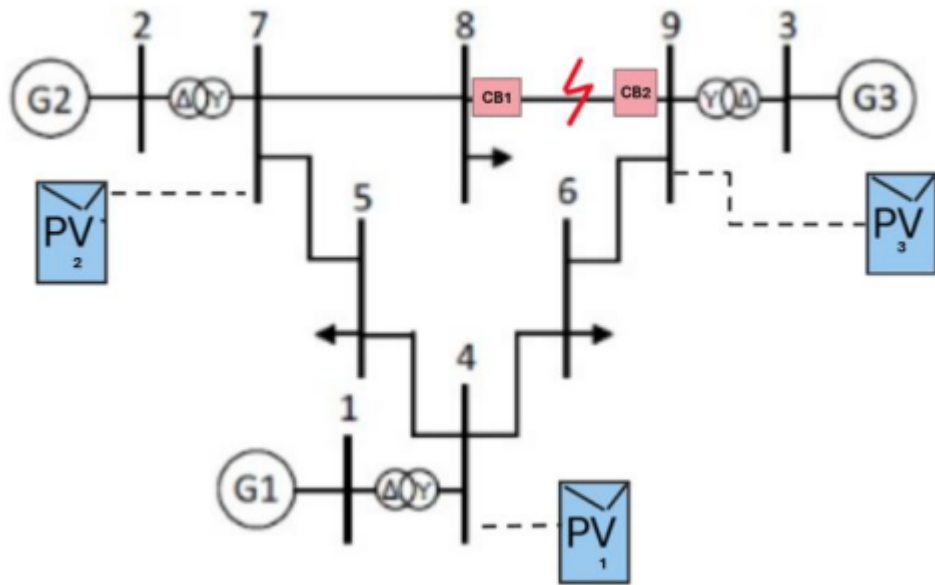


Figure 1. Hybrid IEEE 9 bus system diagrams on RSCAD

Table 1. Default settings of RSCAD IEEE 9 bus system

Bus	Type	V (pu)	PG (MW)	QG (MVA _r)	PL (MW)	QL (MVA _r)
1	SLACK	$1.040 \angle 0.0^\circ$	71.6	27.0	-	-
2	P-V	$1.025 \angle 9.3^\circ$	163.0	6.7	-	-
3	P-V	$1.025 \angle 4.7^\circ$	85.0	-10.9	-	-
4	P-Q	$1.026 \angle -2.2^\circ$	-	-	-	-
5	P-Q	$0.996 \angle -4.0^\circ$	-	-	125.0	50.0
6	P-Q	$1.013 \angle -3.7^\circ$	-	-	90.0	30.0
7	P-Q	$1.026 \angle 3.7^\circ$	-	-	-	-
8	P-Q	$1.016 \angle 0.7^\circ$	-	-	100.0	35.0
9	P-Q	$1.032 \angle 2.0^\circ$	-	-	-	-
From BUS	To BUS		R (pu)		X (pu)	B (pu)
4	5		0.0100		0.0850	0.1760
4	6		0.0170		0.0920	0.1580
5	7		0.0320		0.1610	0.3060
6	9		0.0390		0.1700	0.3580
7	8		0.0085		0.0720	0.1490
8	9		0.0119		0.1008	0.2090

After building the hybrid system, the PV penetration levels of 10%, 40%, and 80% were simulated by varying the PV-to-SG capacity ratio. These cases cover situations from a mostly traditional grid to a scenario where PV is the main source.

2.2. PV inverter modelling

The PV inverter's complex control system is structured through three coordinated layers in RSCAD. The outer control loop is in charge of power setpoints, whereas the inner current control loop ensures very fast waveform regulation. The Phase-Locked Loop (PLL) is the element that stays in exact coordination with the grid frequency. The control system in this case is executing a current-limiting instruction that limits the output to about 1.2 pu within a few milliseconds to the power-electronics-friendly side. We made this a controlled current source driven by custom control logic in RSCAD with a simulation time step of 100 μ s.

2.3. Fault simulation design

Through our RSCAD fault analysis, we investigated the impact of the growing PV penetration on the grid's transient response and this was done by comparing the changes in peak current magnitude, phase-angle shift, and recovery time from one scenario to another. The Fault Logic module was used to introduce faults at time = 0.2 seconds with an impedance of 0.01 pu and the duration varying from 0.1 to 0.15 s. The experiments were carried out for both near-end (busbar) and far-end (line) locations and in all the cases, the time-step resolution was 100 μ s.

Four model configurations (Table 2) evaluate the effects of a different IBR penetration percentages on the system: Case 1, a traditional system with three SGs (0% PV) creating reference fault levels; Case 2, a low penetration, one SG replaced by PV (~22%), the start of the protection challenges; Case 3, a medium-penetration system, two PVs (~45%), the coordination becomes difficult; Case 4, a high-penetration system,

three PVs (~81%), showcasing the composite fault characteristics and the need for more sensitive adaptive settings.

Table 2. Real power output value for all generators in each case

Generators	Case 1 (MW)	Case 2 (MW)	Case 3 (MW)	Case 4 (MW)
SG1	71.6	0	0	0
SG2	163	163	163	57
SG3	85	85	0	0
PV1	0	71.6	71.6	6
PV2	0	0	0	85
PV3	0	0	85	166

2.3.1. Short-circuit fault types

In RSCAD, we simulated three typical faults types to cover all the possibilities. Single-Line-to-Ground (SLG) faults, which typically occur, are the ones that bring in zero-sequence components. Line-to-Line (LL) faults depict the situations of moderate intensity without the participation of the ground. Three-Phase (LLL) faults generate the harshest symmetrical conditions. Such a sequence enabled us to observe how the system behaved at different levels of fault intensity with 100 μ s time resolution.

2.3.2. Simulation parameters and assumptions

Our RSCAD simulations relied on a balanced three-phase model of the system and did not consider secondary effects like temperature changes. A 100 μ s time step, common for all, and a 0.5 s simulation window, long enough to show the complete transient and part of the recovery, were the main features of the simulation.

The adaptive scheme revolves around four pre-configured setting groups in the P3L30 relay. The main idea of adaptation is to gradually decrease the phase overcurrent (51) threshold as the IBR penetration increases, thus reducing the risk of "protection blinding":

- Group 1 (0–25% IBR): Pickup set at 1.5 I_{line} for SG-dominated grids.
- Group 2 (25–50% IBR): Pickup reduced to 1.4 I_{line} to reflect declining fault currents.
- Group 3 (50–75% IBR): Further lowered to 1.3 I_{line} for IBR-majority conditions.
- Group 4 (75% + IBR): Most sensitive setting at 1.2 I_{line} , optionally combined with voltage-dependent timing for security.

The hierarchy shown in Figure 2 effectively balances sensitivity and security as the system changes from typical to high-renewable conditions.

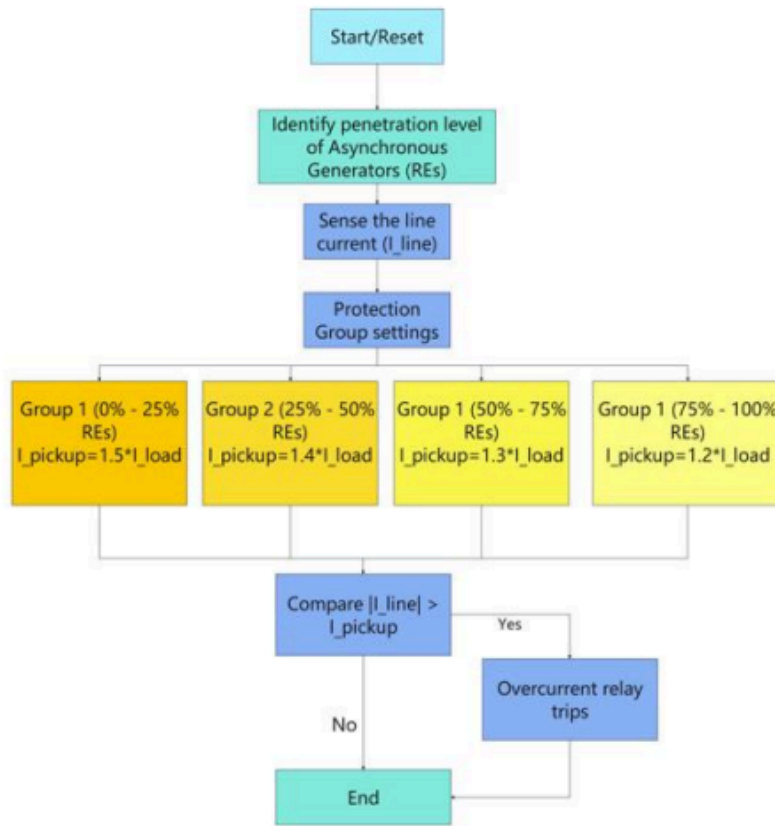


Figure 2. Proposed algorithm for adapting settings

2.3.3. Model validation

RSCAD model accuracy was confirmed in a three-stage manner. First, steady-state checks verified stable pre-fault operation with correct voltages and power balance. Next, dynamic tests exhibited the anticipated SG fault-current surges and the correct PV inverter current limiting. Finally, comparative validation with a pure SG benchmark resulted in deviations of less than $\pm 5\%$, thus confirming that the model is appropriate for further analysis with the 100 μ s time step.

3. Fault current characteristic analysis

In this chapter, fault current characteristics at different PV penetration levels are examined through electromagnetic transient simulations. It looks at the fault current magnitude, waveform distortion, phase angle behaviour, and post-fault recovery. Comparing 0%, 22%, 45%, and 81% PV penetration cases, the main differences in the system transient response due to inverter-based resources are identified.

3.1. Fault current patterns across configurations

The examination of SLG, LLG, and ABC-G faults for the four system configurations yields the same result that the changes caused by increasing IBR penetration to the characteristics of the faults at Bus 8 and 9 are very clear. In fact, the traditional fault current order is maintained most of the time: Three-Phase-to-Ground (LLG) faults are the largest, followed by Double-Line-to-Ground (LLG), with Single-Line-to-Ground (SLG)

faults being the smallest, shown in Table 3 to 5. Nevertheless, the absolute current values and their relative reduction differ considerably with higher IBR penetration.

Table 3. Fault currents based on phase a to ground fault

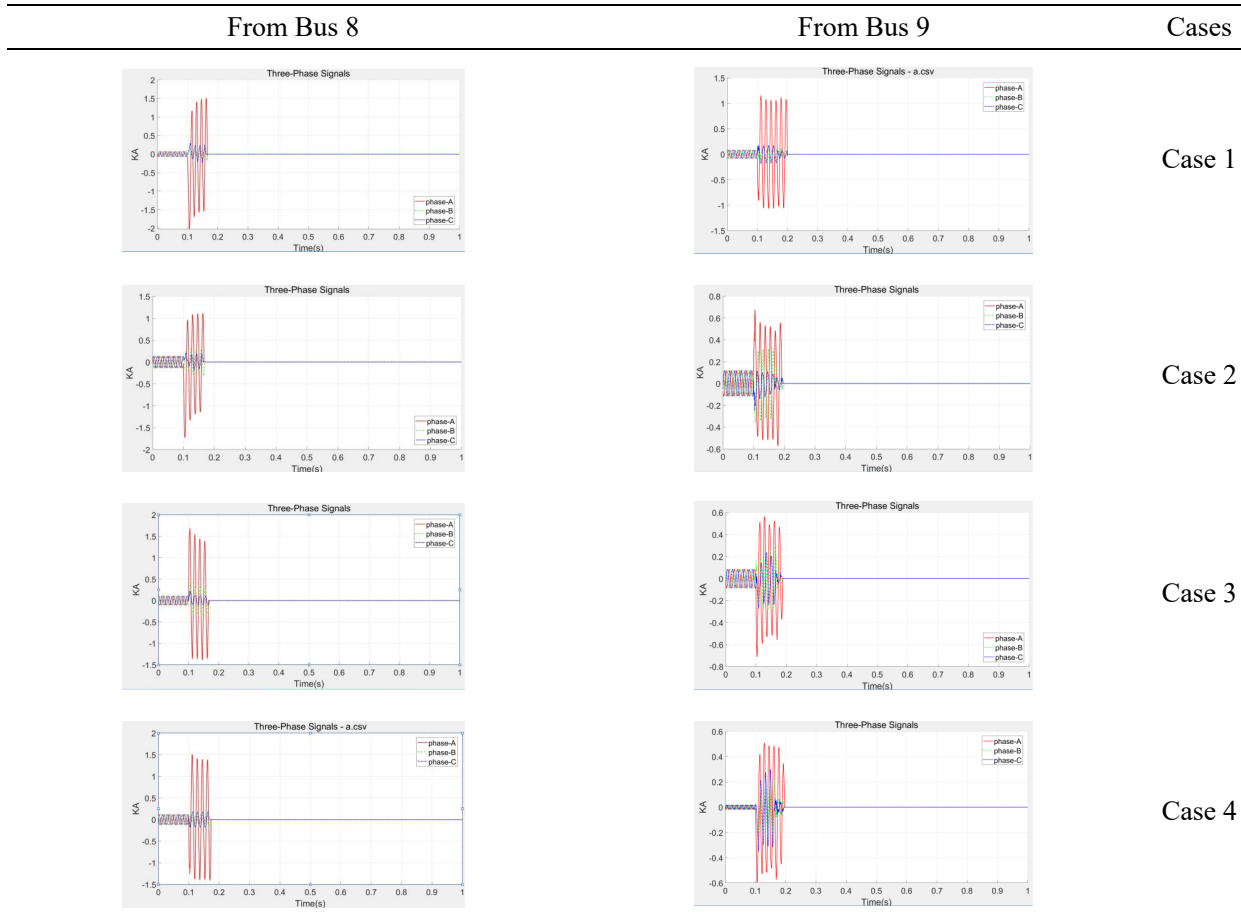


Table 4. Fault Currents Based on Phase AB to Ground Fault

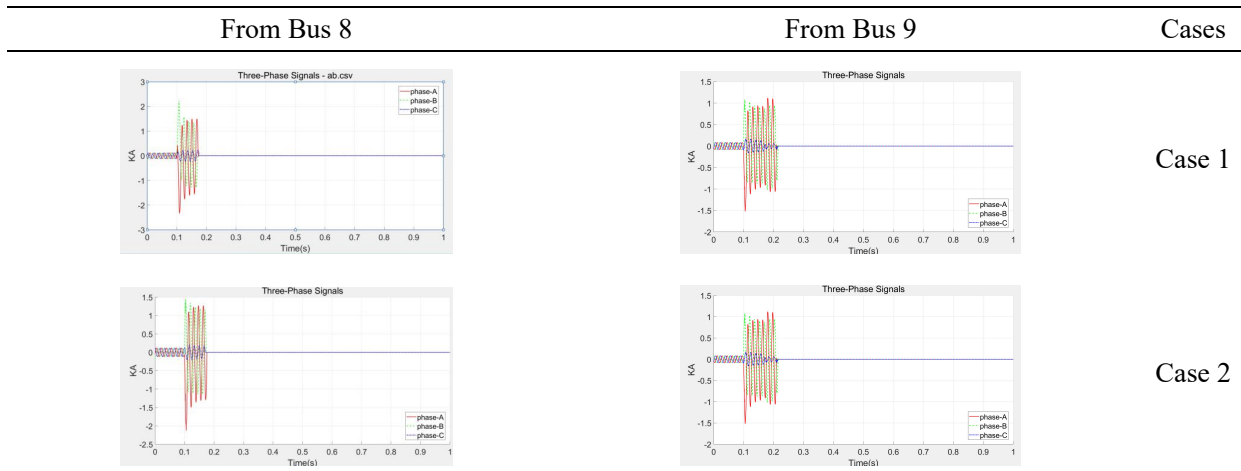
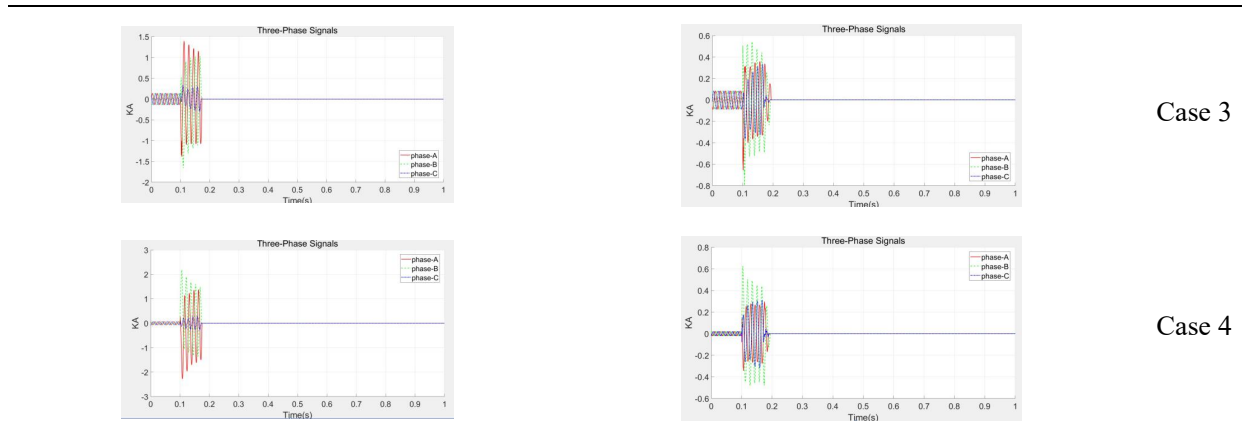
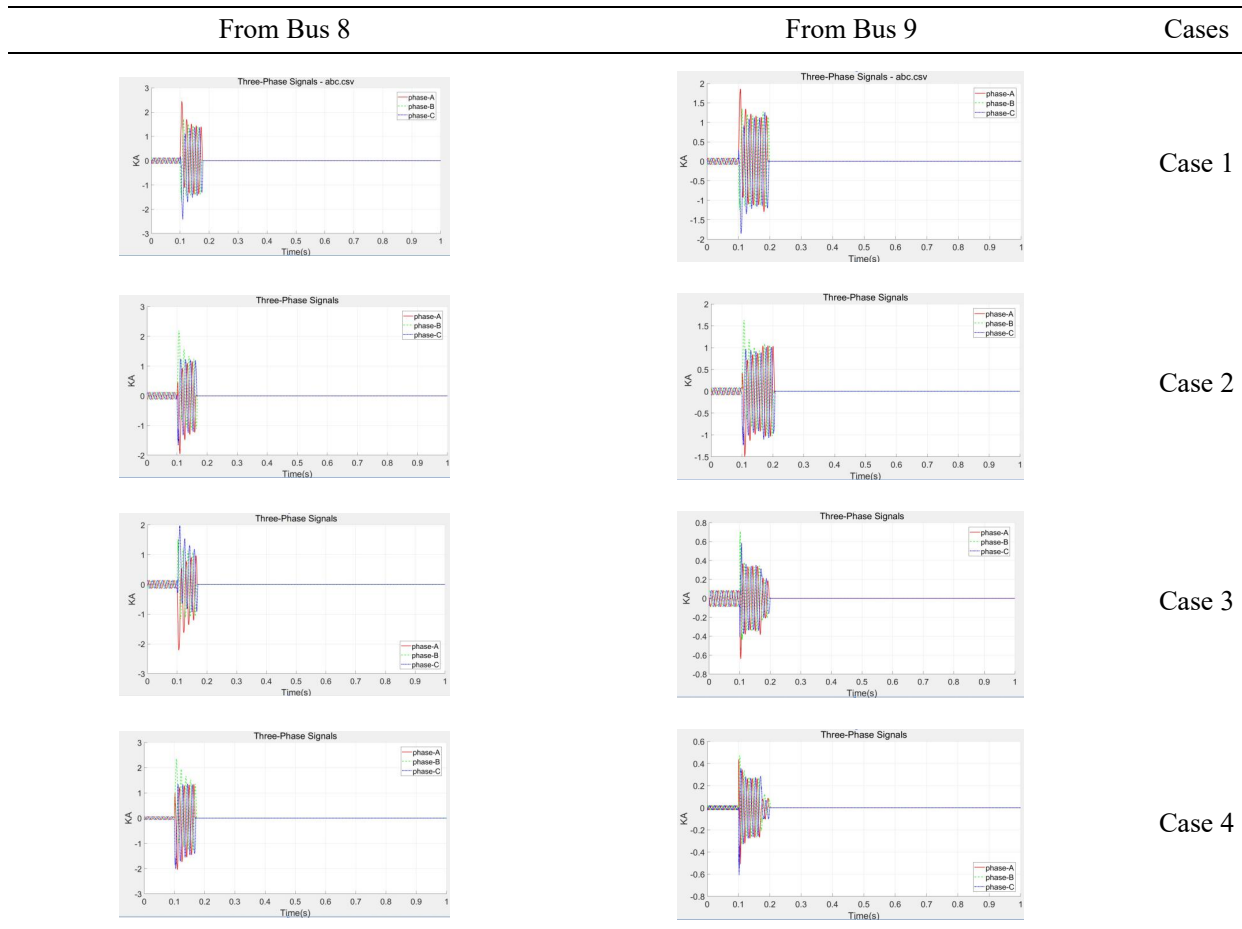


Table 4. Continued**Table 5.** Fault currents based on phase ABC to ground fault

Bus 8 is the one that maintains almost the same fault current that is able to go through the PV penetration levels due to the fact that it is very close to the slack bus with the big SGs that provide a low-impedance path and high short-circuit power, thus keeping the LLLG > LLG > SLG hierarchy intact.

At Bus 9, the change of SGs to current-limiting inverters reduces the fault current significantly, however, the contributions of the remote slack-bus SG still make it detectable, thus protection blinding avoided, and the relay settings can be adapted, becoming more sensitive.

3.2. Fault voltages

The investigation of voltage changes during fault situations shows that these changes are quite different in the case of the traditional systems and high-PV penetration systems. Voltage at both Bus 8 and Bus 9 dropped drastically during the fault condition in all system configurations, which is evident from Table 6-8. The intensity of the voltage depressions depended on the fault type and system strength: in Single-Line-to-Ground (SLG) faults the voltage went down to 0.6-0.8 pu range most of the time, whereas in the case of the more severe Three-Phase-to-Ground (LLLG) faults the voltage dropped even further to 0.15-0.3 pu.

Table 6. Bus voltage waveform during a to ground fault

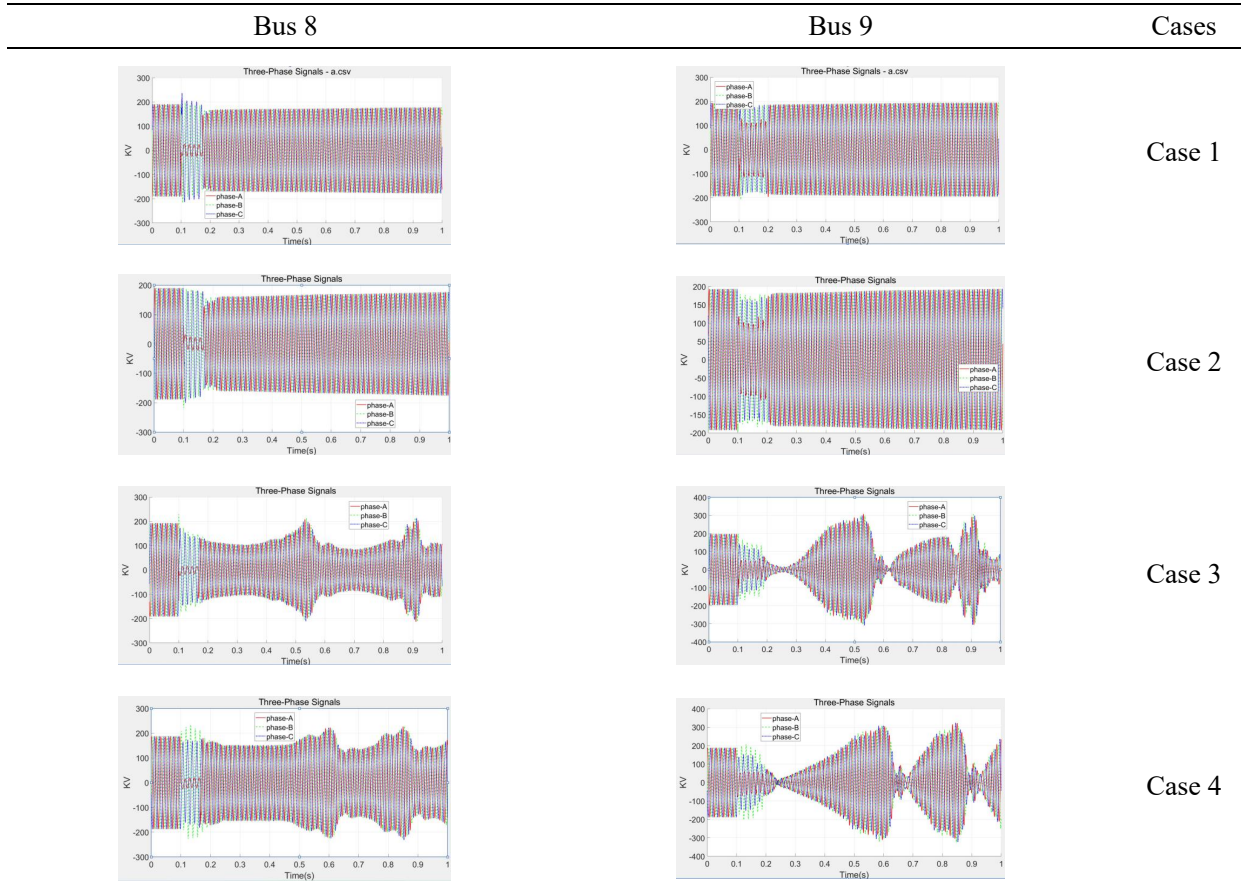


Table 7. Bus voltage waveform during AB to ground fault

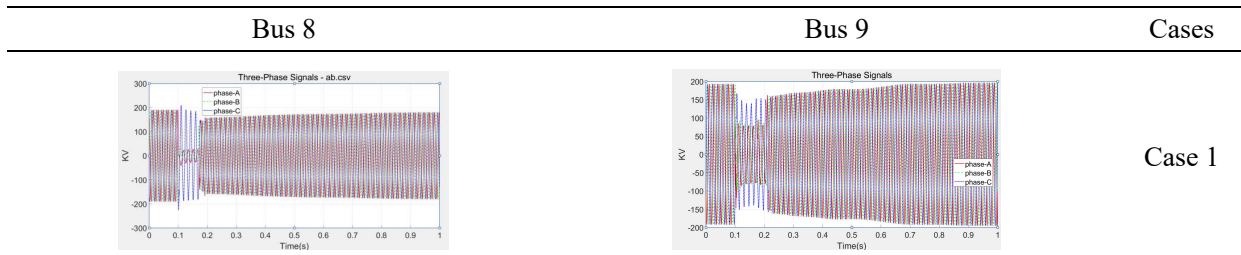
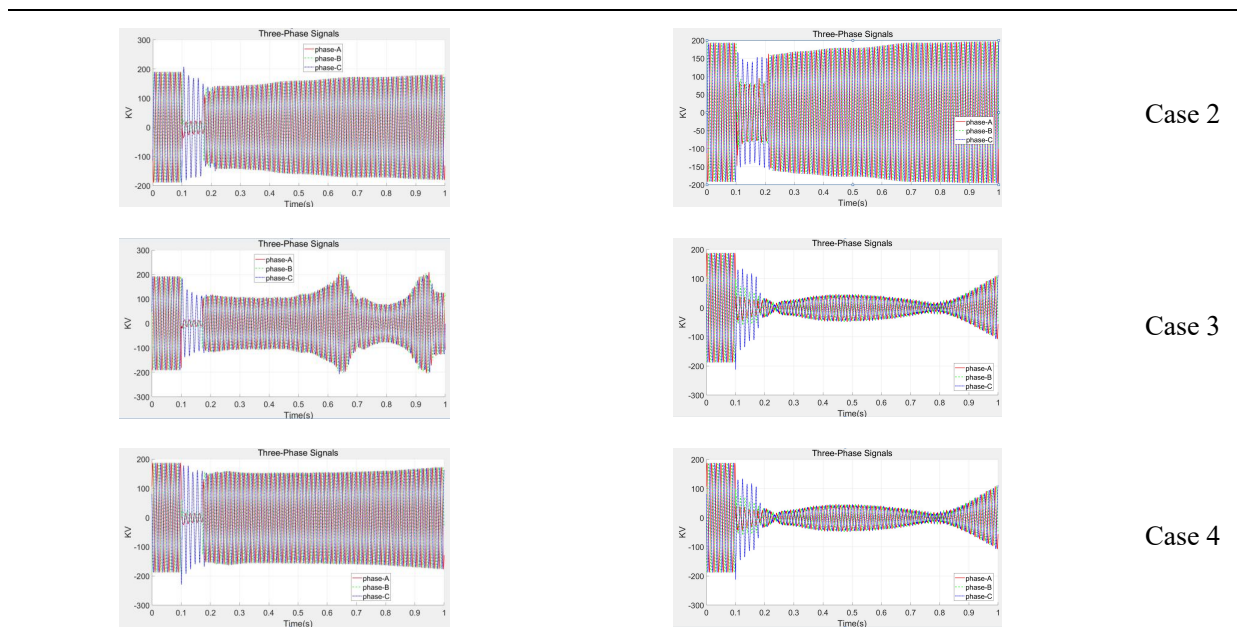
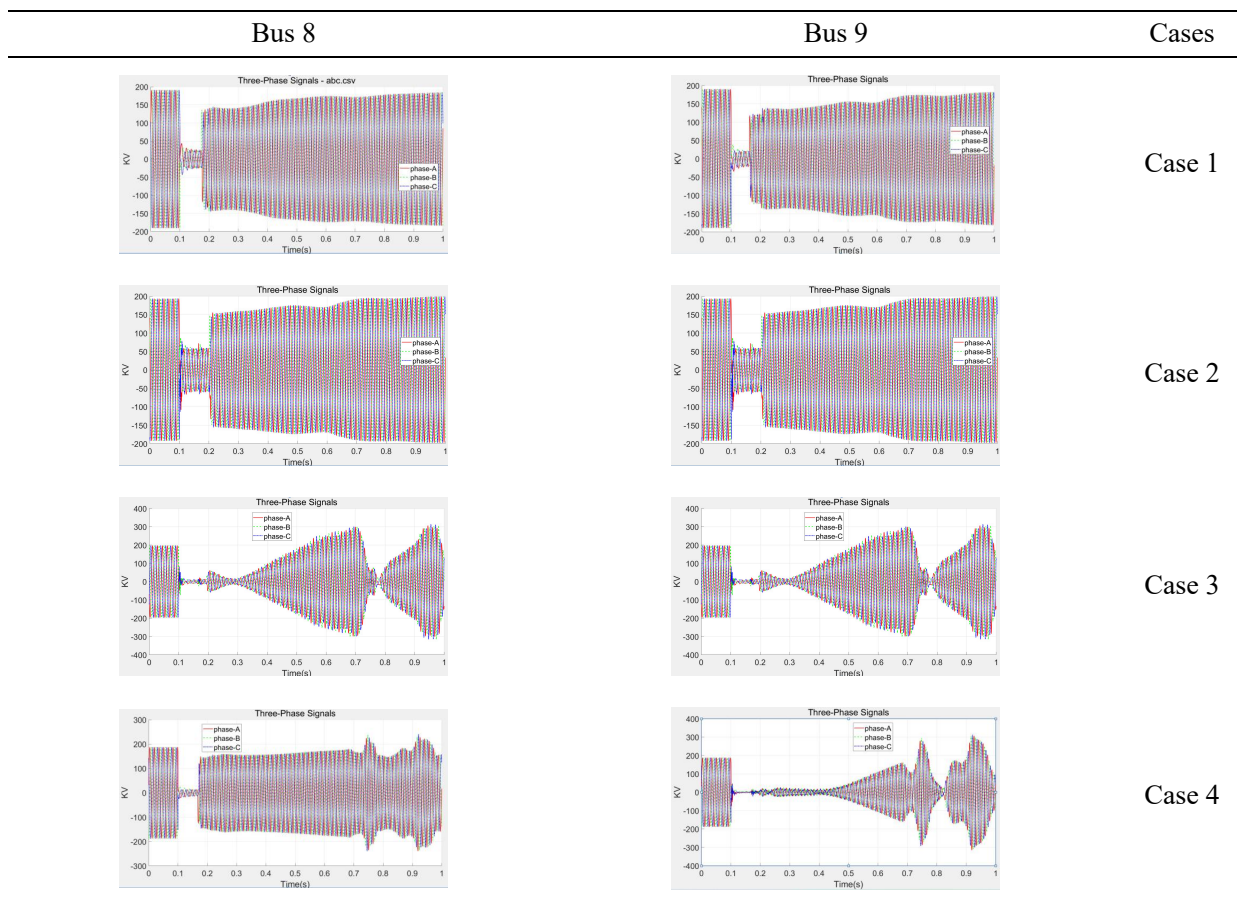


Table 7. Continued**Table 8.** Bus voltage waveform during ABC to ground fault

Conventional systems with little or no PV show a strong post-fault voltage recovery in which the voltage returns to normal within 10-15 cycles due to the inertia of the synchronous generator and voltage regulation. In the case of high PV penetration, the oscillations last for 30-40 cycles and the deviations from the norm are large, which indicates that the damping is reduced and there are complex inverter-control interactions.

The increased dynamics make the system less resistant to disturbances and the only way to operate the system safely and reliably under stress is to use advanced grid-forming controls and implement stronger stability measures.

3.3. Fault injections from PVs

Most of the power system faults involve fault currents from PV systems that are fundamentally different from those caused in other power systems during disturbances. Synchronous generators usually inject 5-10 times their rated current during faults, whereas grid-following PV inverters limit the fault current to about 1.2-2.0 times the rated current, as seen in Table 12-14 [5]. Although this protective action helps to avoid a lethal overcurrent and thus protects the inverter hardware, it makes the malfunction coordination and the system recovery process much more difficult.

Table 9. Fault currents detected from PV1 based on A to ground fault

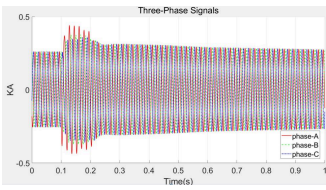
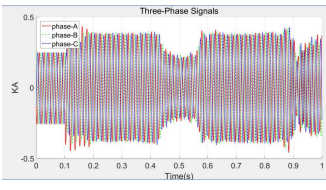
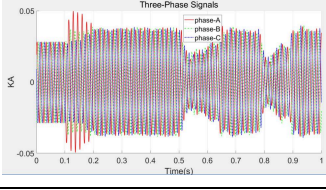
Case	Fault Current Waveform
Case 2	
Case 3	
Case 4	

Table 10. Fault currents of PV1 based on AB to ground fault

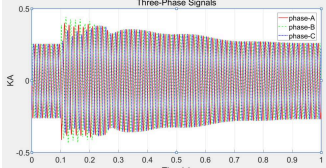
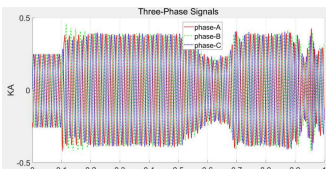
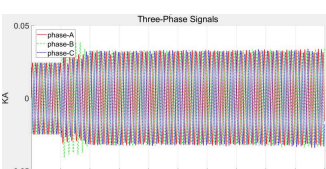
Case	Fault Current Waveform
Case 2	
Case 3	
Case 4	

Table 11. Fault currents of PV1 based on ABC to ground fault

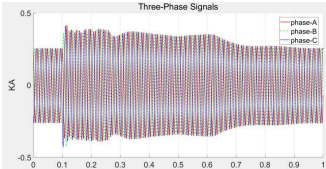
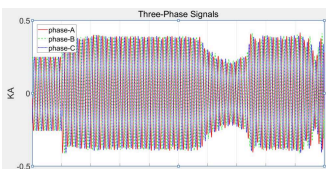
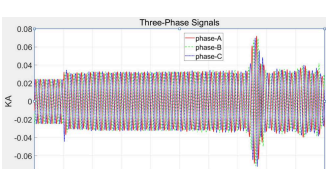
Case	Fault Current Waveform
Case 2	
Case 3	
Case 4	

Table 12. Fault currents detected from PV2 based on B to ground fault

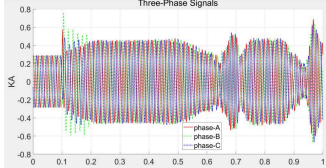
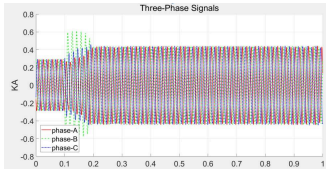
Cases	Fault Current Waveform
Case 3	
Case 4	

Table 13. Fault currents of PV1 based on AB to ground fault

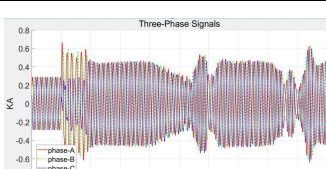
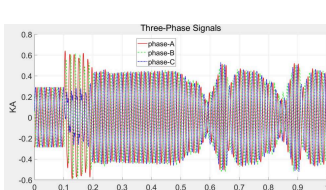
Cases	Fault Current Waveform
Case 3	
Case 4	

Table 14. Fault currents of PV1 based on ABC to ground fault

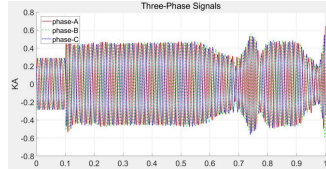
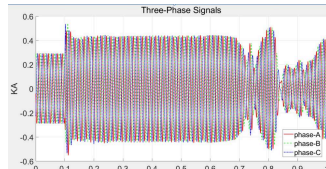
Cases	Fault Current Waveform
Case 3	
Case 4	

Table 15. Fault currents detected from PV2

Case4	Fault Current Waveform
B to Ground	
AB to Ground	
ABC to Ground	

Limited Photovoltaic (PV) fault currents result in slower, oscillatory post-fault recovery due to reduced inertia and complex three-phase inverter interactions. However, the protection strategy presented in this paper was effective in isolating faults, as confirmed by the synchronous generator that was retained and therefore, with enough synchronous or grid-forming support, existing protection can be adapted through settings to allow high-renewable operation.

4. Protection impacts and adaptive setting strategies

This chapter, based on the fault analysis in Chapter 3, considers the effects of a protection system response when there is a high penetration of PV. It fleshes out the adaptive tactics for keeping the system functioning dependably by addressing the difficulties arising for the principal protection functions, suggesting the feasible solutions taken from the system behaviour that has been observed.

4.1. Protection performance under high PV penetration

Higher PV penetration causes the short-circuit strength to be lower and the protection challenges to be multiple [6]. The diminished fault current contributions of synchronous generators may lead to fault currents falling below the pickup thresholds, especially at remote buses, whereas the inverter current limiting may change the waveforms and worsen the phasor estimates.

Both directional and distance elements suffer from decreased reliability because of low zero-sequence content, angle shifts caused by PLL, overestimation of impedance, unstable R-X trajectories, and shorter fault durations, thus making fixed settings being insufficient at different penetration levels [7].

4.2. Adaptive protection mechanism

In order to keep the protection sensitivity at different PV levels, the P3L30 relay carries out an adaptive overcurrent scheme with four setting groups. As the support of the synchronous generator decreases, the

pickups lower from 1.5 to $1.2 \times I_{\text{line}}$, thus improving sensitivity in weak grids and maintaining security is kept when normal sources are still online.

The adjustment on a real-time basis reflects the number of PV units that are active and this is RSCAD 4-bit signal which is passed via Gigabit Transceiver Digital Output (GTDO) outputs to the appropriate group to be selected by the relay. The results of the simulations indicate that the presence of even one SG is enough to raise the short-circuit levels and improve the relay performance under high PV penetration [8].

5. Conclusion

This research addressed the issues of protection in a system with a high percentage of Photovoltaics (PV). It was found that inverter-based resources emit very limited fault currents that rapidly decay, thus posing the risk of protection devices becoming "blind". A four-group adaptive overcurrent scheme was created, which by lowering the pickup from $1.5I_{\text{line}}$ to $1.2I_{\text{line}}$ as PV penetration increased, was able to keep consistent operation in all the cases tested. The simulations also showed a non-linear decrease in fault current and verified that keeping one synchronous generator helps to maintain system strength. The scenarios with high PV showed slower post-fault recovery and voltage oscillations, thus implying the necessity for better grid-forming controls. Although the scheme was verified through manual operations in RSCAD, the upcoming work should be dedicated to full automation.

References

- [1] Tuladhar, L. R., & Banerjee, K. (2019, November). *Impact of the penetration of inverter-based systems on grid protection*. In CIGRE US National Committee 2019 Grid of the Future Symposium. https://cigre-usnc.org/wp-content/uploads/2019/10/2D_3.pdf
- [2] Muenz, U., Bhela, S., Xue, N., Banerjee, A., Reno, M. J., Kelly, D. J., Farantatos, E., Haddadi, A., Ramasubramanian, D., & Banaie, A. (2024). *Protection of 100% inverter-dominated power systems with grid-forming inverters and protection relays: Gap analysis and expert interviews** (Report No. SAND-2024-04848). Sandia National Laboratories. <https://doi.org/10.2172/2429968>
- [3] El-Sayed, W. T., Azzouz, M. A., Zeineldin, H. H., & El-Saadany, E. F. (2020). A harmonic time-current-voltage directional relay for optimal protection coordination of inverter-based islanded microgrids. *IEEE Transactions on Smart Grid*, 12(3), 1904–1917. <https://doi.org/10.1109/TSG.2020.3044350>
- [4] Jia, K., Yang, Z., Fang, Y., Bi, T., & Sumner, M. (2019). Influence of inverter-interfaced renewable energy generators on directional relay and an improved scheme. *IEEE Transactions on Power Electronics*, 34(12), 11843–11855. <https://doi.org/10.1109/TPEL.2019.2904715>
- [5] Meskin, M., Domijan, A., & Grinberg, I. (2020). Impact of distributed generation on the protection systems of distribution networks: Analysis and remedies – review paper. *IET Generation, Transmission & Distribution*, 14(24), 5944–5960. <https://doi.org/10.1049/iet-gtd.2019.1652>
- [6] Qays, M. O., Ahmad, I., Habibi, D., Aziz, A., & Mahmoud, T. (2023). System strength shortfall challenges for renewable energy-based power systems: A review. *Renewable and Sustainable Energy Reviews*, 183, 113447. <https://doi.org/10.1016/j.rser.2023.113447>
- [7] Shazon, M. N. H., & Jawad, A. (2022). Frequency control challenges and potential countermeasures in future low-inertia power systems: A review. *Energy Reports*, 8, 6191–6219. <https://doi.org/10.1016/j.egyr.2022.04.063>
- [8] Velásquez, R. M. A., & Velásquez, R. F. A. (2025). Enhanced fault detection in zig-zag transformers: Insights from dissolved gas analysis and transient current analysis. *Results in Engineering*, 25, 104166. <https://doi.org/10.1016/j.rineng.2025.104166>